A series of detector system for MUSE

J.L. Lizon*[(1)], C. Dupuy[(1)], M. Accardo[(1)], R. Reiss[(1)], S. Deiries[(1)], R. Hinterschuster[(1)]
T. Fechner[(2)], A. Kelz[(2)], S. Mudit[(2)], O.Streicher, P. Weilbacher[(2)]

[(1)] European Southern Observatory (ESO), Karl-Schwarzschild-Strasse 2, 85748 Garching bei München, Germany
[(2)] Leibnitz-Institut fuer Astrophysik Potsdam (AIP), An der Sternwarte 16, 14482 Potsdam, Germany

ABSTRACT

The 24 IFU from MUSE are equipped with 4K x 4K CCD detectors which are operated at cryogenic temperature around 160 K. The large size of the chip combined with a rather fast camera (F/2) impose strong positioning constrains. The sensitive surface should remain in an angular envelope of less than 30 arc sec in both directions. The ambitious goal of having the same spectrum format on every detector imposes also a very accurate positioning in the image plane. The central pixel has to be located in a square smaller 50 microns relative to the external references.
The first part of the paper describes the mechanical design of the detector head. We concentrate on the various aspects of the design with its very complex interfaces. The opto-mechanical concept is presented with an emphasis on the robustness and reliability. We present also the necessary steps for the extreme optimization of the cryogenic performance of this compact design driven with a permanent view of the production in series.
The techniques and procedures developed in order to meet and verify the very tight positioning requirements are described in a second part. Then the 24 fully assembled systems undergo a system verification using one of the MUSE spectrographs. These tests include a focus series, the determination of the PSF across the chip and a subsequent calculation of the tip/tilt and shift rotation of the detector versus the optical axis.

Keywords: Optical instrument, Detector, Optical alignment

1. INTRODUCTION

MUSE, the Multi Unit Spectrograph Explorer instrument is one of the next instruments to be installed in the coming months onto the VLT. MUSE combines 24 spectrographs in order to be able to probe a field of view as large as possible. Each spectrograph is equipped with 4000 x 4000 pixel detectors. If ESO has a large and long experience in building detector system (since the first CCD detector installed at La Silla on 1983), it is the first time we faced such a high number of discrete detector systems. The actual Detector Head was developed more than 10 years ago for the VLT and was designed to be versatile allowing the accommodation of a large variety of chips. This was the best opportunity to design a new well suited detector head fully optimized for this specific application.

2. DETECTOR HEAD DESIGN

Figure 1 shows an overall view (exploded view and cut through) of the detector head. An important effort has been done in order to compact the head as much as possible. Both the thermal load and the out-gassing are significantly reduced with the limitation of the area of the warm surfaces. The number of parts has also been reduced to the strict minimum.

From the principle the design is following the traditional approach with a cold bench (1) coupled to the warm front flange (2) via four insulating plates (3) made of epoxy glass fiber material. MUSE being a static instrument there is no real conflict between the thermal conductance and the mechanical stability. The insulating plates carry also the intermediate relay where the back part of the radiation shield (4) is thermally connected to the front shield (5). The thermal connection system developed for the standard VLT heads has been used again. The continuity between the cryostat and the head is ensures via spring loaded thermal contact for both the radiation shield (not shown on the figure) and the detector cooling (6).

*jlizon@eso.org; phone 0049 8932006780; fax 0049 8932006457; www.eso.org

This allows a very easy separation of the two sub-systems without worrying about thermal braid connection. The electronic board used to put in form the signal of the CCD has been designed in order to fit with the internal geometry of the detector head. It is attached onto two of the walls of the connector flange and receives directly the connection from the chip flexible cables.
The most novel aspect of the design is the addition of the adjustment flange (7). This flange ensures on the front side a perfect interface between the Window Field Lens (8) and the spectrograph using a double three pins/slot combination. The back side of this flange is machined on demand according to the alignment measurement. This allows positioning of the CCD sensitive area within the tight requirement of the project.
The interfacing of the Field Lens has been intensively discussed and agreed with the optical company in charge of the spectrograph. The final barrels have been supplied to the optical company in order to be sure about the compatibility with the vacuum and cryogenic environment. As usual a highly polished warm radiation shield (9) is used to limit the thermal emitting area of the window to the optical clear aperture of the lens.

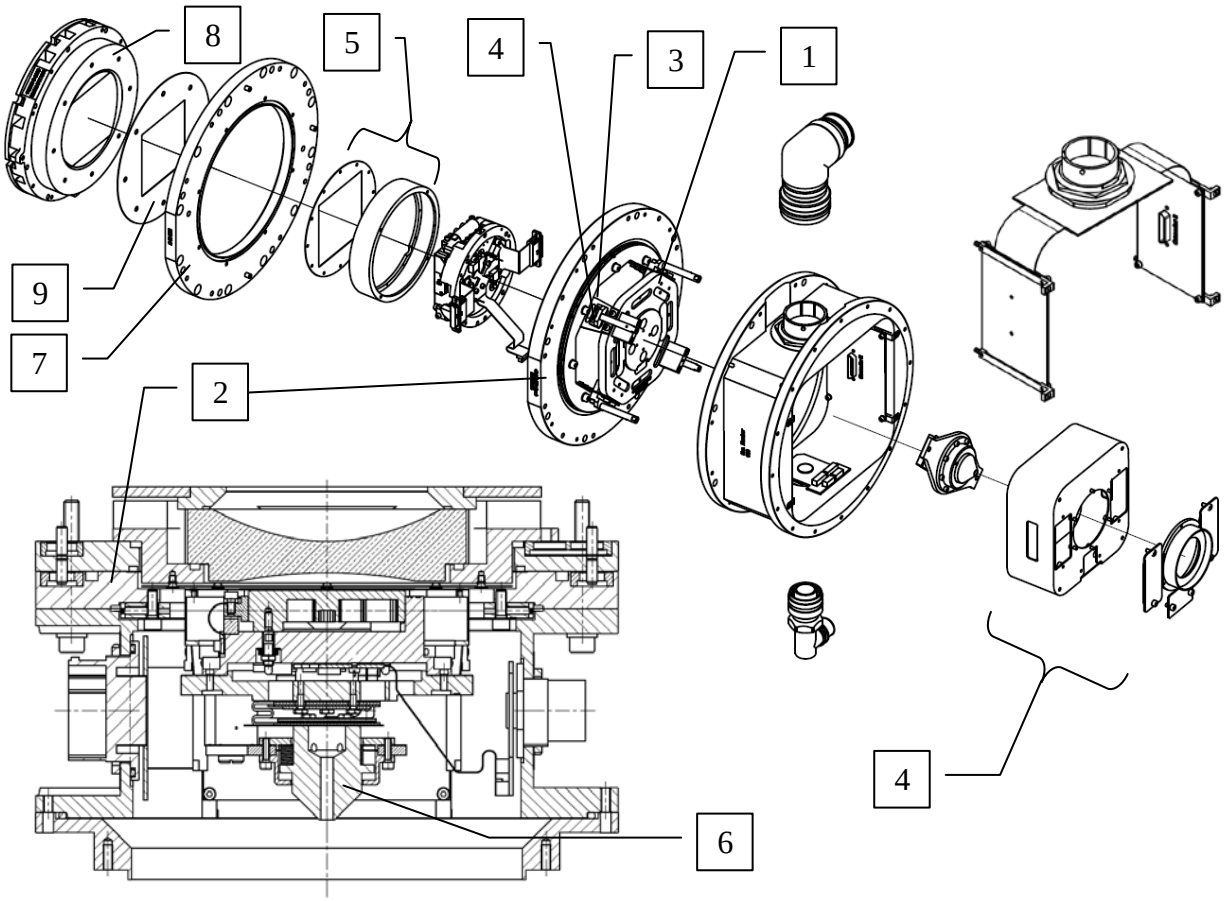

Figure 1: Overall view of the Detector Head

Figure 2 shows the detail of the CCD detector chip mounting. The chip is clamped onto its chip carrier (10) with a controlled force using spring washers (11). This defined the chip position along Z and allows for the required motion freedom to adapt the differential thermal expansion. This clamping is not enough to ensure the heat sinking of the chip. The thermal connection is mostly provided by the “Y” referencing and fixation system. The pressure plate (12) pushes the chip onto the reference of the chip carrier. A second pushing point (13) is used to define and fix the position along (X). The surfaces of the chip carrier as well as the one of the pressure plate are gold coated in order to optimise the thermal conductance. A conducting copper foil (14) is used to heat sink the pressure plate.

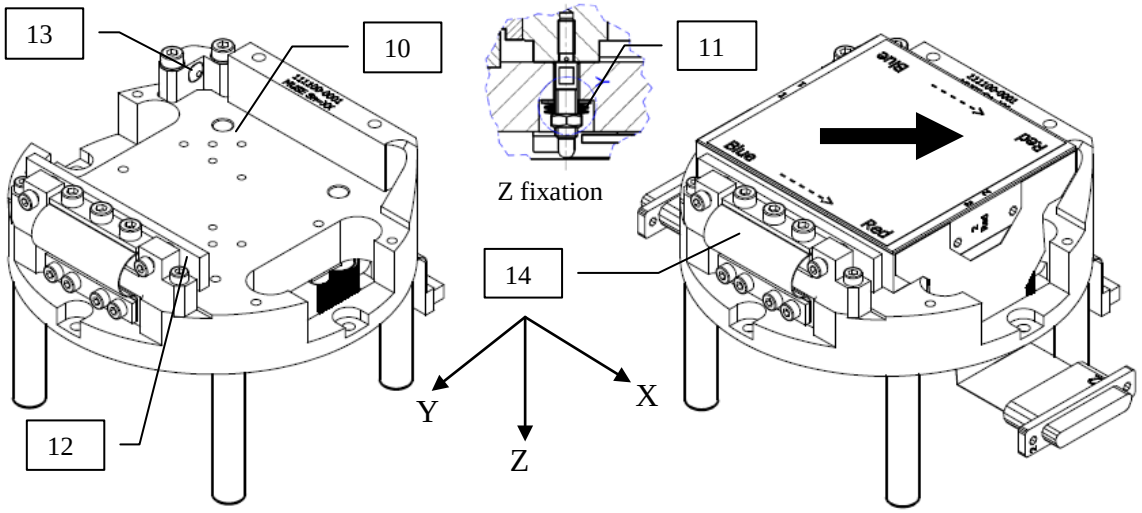

Figure 2: Mounting of the CCD chip

The clamping of the chip is all based on pre-determined stored forces which only need to be liberated by unscrewing screws. This allows reducing considerably the stress on the detector specialist during the installation phase. There is no risk to apply too high force and to introduce irreversible mechanical damages to the detector.

3. DETECTOR HEAD INTEGRATION

The integration of the first four units has served elaborating a detailed assembly procedure. This procedure includes a high level of details like the tightening torque for every screw. This document is also supported by a checklist with various verifications to be documented and included in the delivery folder which follows every detector system. This documentation has been used intensively by our partner from AIP (Astronomy Institute Potsdam) who performed the integration of the Detector Head series. In addition this has ensured a very high level of quality over the complete integration process what is not always the case for such routine tasks.
Among the various dedicated facilities we can mention the specific reference tool which has been designed for the assembly of the cold/warm bench system in order to guarantee a perfect relative positioning of the two components. This device is used to hold in position the two main parts during the clamping of the insulating plates. This positioning has been verified for every head. For this operation the chip is replaced by a dummy chip. The position of this dummy (7 points marked with green letters on figure 3) is measured on a 3D measuring machine.
The integration operations entirely carried out in clean room, the head left the clean room only after closing with a dummy window flange and a special cryostat interface flange for the final leak testing. Once the fully integrated DH received at ESO one additional testing step has been added. The heads have been integrated to the dedicated cryostat and a full thermal cycle has been carried out before integration of the real CCD chip.

4. METROLOGY AND ADJUSTMENT

The very strong requirements on the absolute positioning of the chip on the optical axis are presented in table 1 and figure 3. They can be explained and justified as follows:

- dZ, dΘX and dΘY → guarantee the optimal optical quality all over the chip
- dX, dY and dΘZ → guarantee the same spectrum format and the full spectral coverage for the 24 spectrographs

From the beginning it has been clear that there is no real way to achieve directly these requirements. Therefore the additional adjustment flange described in chapter 1 was added. A dedicated measuring procedure has been developed in order to characterize the position of the active surface relative to the front flange. This procedure is based on the use of the Chip Position Measuring Machine (CPMM) which is shown on figure 4. The CPMM is based on a set of 5 small

projectors (1) producing images of the center and on the four corner of the chip. The projector is a simple optical system build from commercially available lenses. It produces a direct image of an optical fiber (3). A computer controlled translation stage (3) is used to scan along the optical axis allowing through focus exploration in five points. The machine reproduces the full interface of the spectrograph including the position reference pins (5). For this measurement which is carried out in the normal operating conditions (DV evacuated and cryostat cold) the detector head is sealed using a flat parallel test window (4).
A number of iterations have been necessary in order to optimize the components (Optical fiber, light source…) and the procedure (steps, scanning direction…). Also the interfacing procedure (CPMM on DH) required a clear definition including well defined and controlled tightening of the fixation screws.

dX	15 µm	dΘX	0.5 arcmin
dY	15 µm	dΘY	0.5 arcmin
dZ	10 µm	dΘZ	1 arcmin

Table 1: Chip position requirement

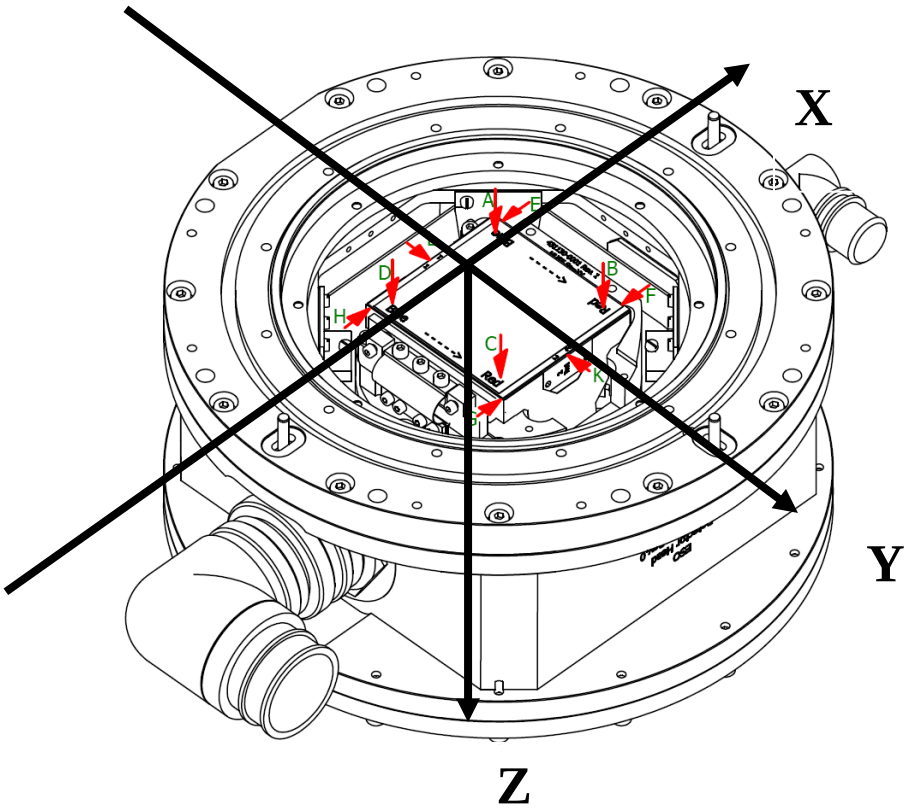

Figure 3: Chip position requirements

A special routine has been developed in order to automate the measuring operation. The operation which is fully computer controlled carries out the complete measuring sequence (Take an exposure, acquires the data, move the Translation Stage to the next position, take the next exposure...), reduces the images and delivers the five through focus curves as well as the real position of the CCD sensitive surface. These results shown in figure 5 are directly used by the sub-program to define the final shaping of the adjustment flange. After manufacturing the adjustment flange is installed on the DH and an additional verification is carried out. Only when this step is passed the field lens can be installed and the detector system is ready for the next verification.

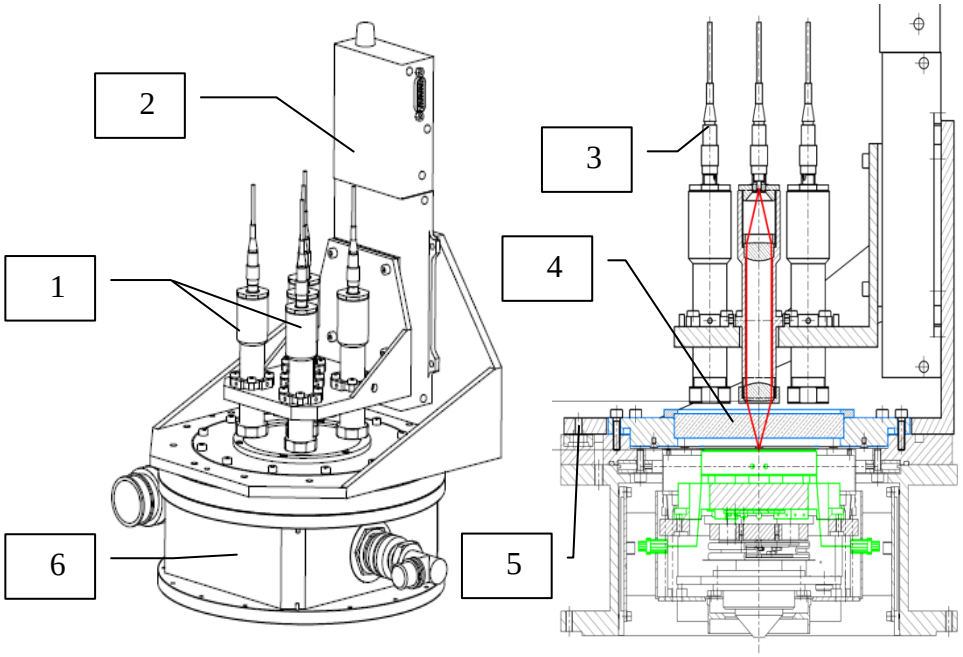

Figure 4: Chip Position Measuring Machine (CPMM)

1. Projectors, 2. Translation stage, 3. Optical fibres, 4. Flat/parallel test window, 5. Reference pins, 6. Detector Head

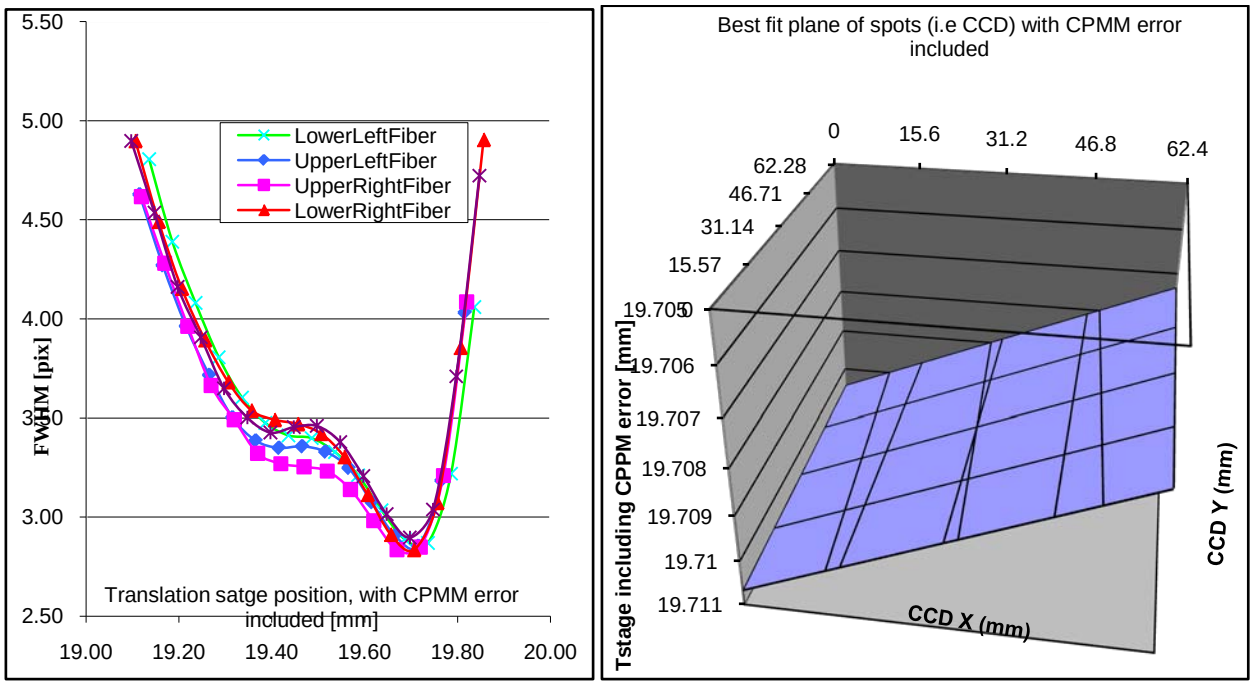

Figure 5: Through focus curves (left) and CCD sensitive surface position (right)

After the first 10 systems an improvement has been brought to the method. The first measurement for the definition of the adjustment flange has been carried out with a reference flange. Using the CPMM always close to the same focus position avoids the measurement to suffer from calibration problems.

5. TESTING, PERFORMANCE

5.1 Aim and Purpose

Once completed, the detector vessel (DV) sub-system is send from ESO to the AIP for further system verification. The aim of the system test is to measure the performance and overall alignment of the detectors when mounted at the MUSE spectrograph [1], including all optical elements as the field lens window acts both as Dewar window and as the last optical element of the spectrograph. For each detector the image quality is measured across the chip (i.e. in spatial and spectral direction), the tip/tilt alignment with respect to the optical axis is determined and the relative shift and rotation calculated. In addition to the individual results, the serial testing of altogether 25 detector systems, using a single test bench yields the distribution of the measured parameters and indicates the achievable re-production accuracy for the system. Ideally, the MUSE detector systems can be made so similar, that they perform within specification at any of the 24 spectrographs and if needed can be interchanged without any re-alignment or re-adjustments.

5.2 Detector test bench setup

The detector test bench (Fig. 6) consists of a MUSE spectrograph system (SPS), a specialized illumination unit (IU) with light sources and the detector vessel (DV) under test plus auxiliary electronics, controllers and shutter.

The illumination unit features a laser-drilled precision pinhole mask (of 11 pinholes with 10 microns diameter) and a pupil mask with elliptical apertures. The pinholes are not resolved and thus the point-spread-function of the optical system is measured (Fig. 7). The elliptical pupil masks restrict the input beam to F/4 and F/8 respectively, identically to the output of the MUSE image slicer system (ISS). Similar to an integrating sphere, the IU provides an uniform illumination of the pinholes. The light of various lamps can be fed into the IU, while a shutter controls the exposure time. The lamps are the same as in the MUSE calibration unit [2], namely a Halogen continuum source and Mercury (Hg), Neon (Ne) and Xenon (Xe) spectral lamps. The whole unit is mounted onto a motorized z-translation stage, so that the object plane (i.e. the pinhole mask) can be moved through focus in front of the collimator.

The spectrograph with serial number 3 (SPS3) is used in the test bench and acts as reference for (almost) the entire DV-acceptance test series. The MUSE spectrographs are produced in series by the company Winlight and are validated at CRAL [3]. The ESO MUSE team delivered the completed detector vessels and a set of periphery equipment, such as the New Generation Controller (NGC), a “TeePee” controller and a local control unit (LCU) to operate the CCDs.

Using the first detector vessels (DV02 and DV04), the entire test bench was validated. In particular the stability and repeatability of the setup was investigated. The detector was dis- and re-mounted several times, sometimes with different orientations, or with different loads applied. The validation also included deliberate tilts or shifts of either the illumination unit or the detector system as to detect these offsets. Long time series were done to verify the stability of the setup.

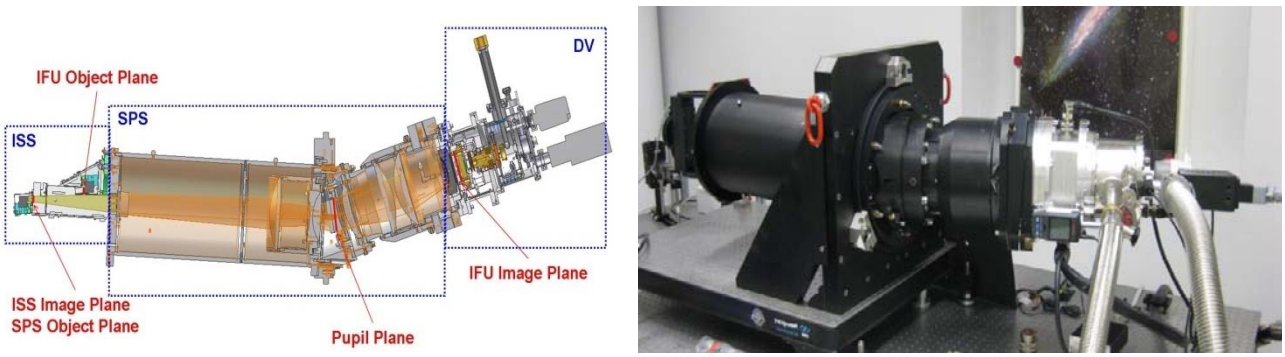

Figure 6. Left: CAD view of a MUSE integral field unit (IFU). For the DV acceptance testing, the image slicer subsystem (ISS) is replaced with a pinhole illumination unit (IU). Right: The detector test bench at AIP (without baffles and light sources). The detector under test (right) is mounted to a MUSE spectrograph (center). At the collimator side of the spectrograph (left) an illumination unit provides a set of pinholes in the object plane.

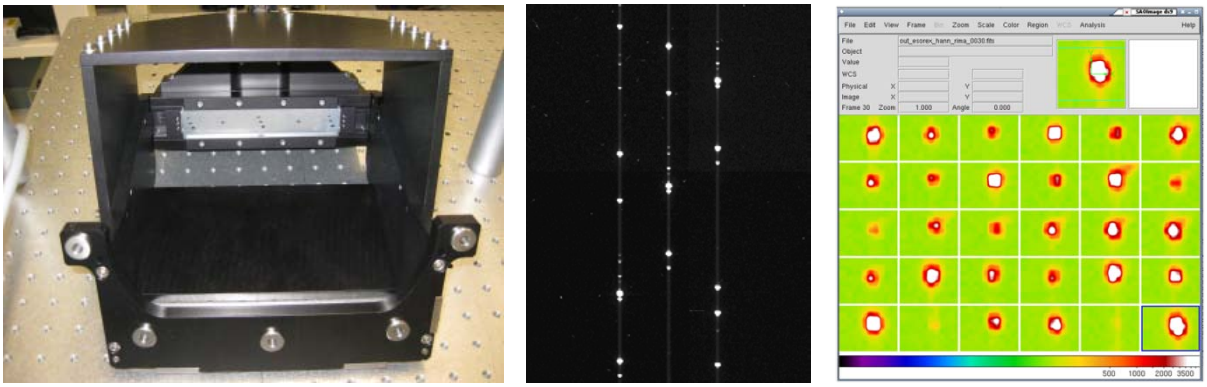

Figure 7. Left: view onto the illumination unit with pinhole and pupil masks. Center: section of the raw CCD data showing the PSFs created by 3 pinholes (horizontal) across wavelength (vertical direction) using Mercury and Neon spectral lamps. Right: display of enlarged and interpolated arc spots to calculate the ensquared energy of the PSF.

5.3 Test procedures and focus series

After pumping (typically 10^{-5} to 10^{-6} mbar) and cooling (to 163 K), long darks (of 30 to 60 minutes) were taken. Additional flat field exposures (with integrating sphere in front of DV, Fig. 8) or spectral flats (DV at spectrograph, illuminated with continuum lamp) were taken. This data, together with the tests done at ESO-ODT, is used to characterize the specifics of each detector and the information is also fed into the data reduction pipeline.

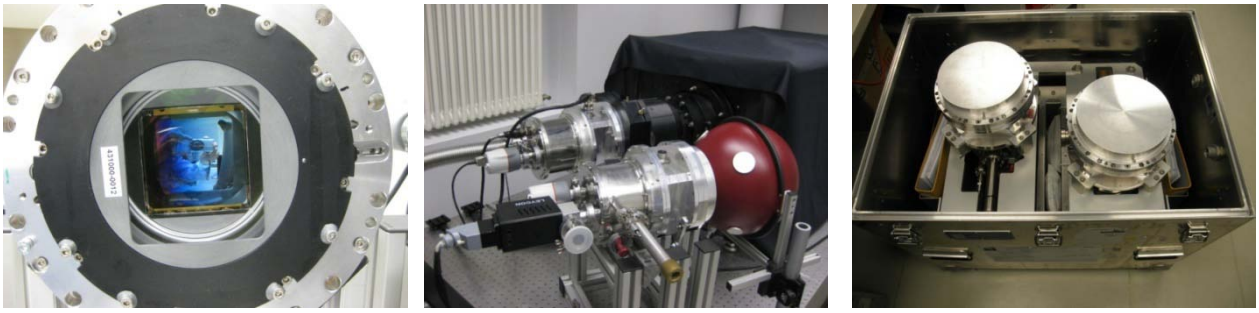

Figure 8. Left: visual inspection of detector and graded-index coated field lens window. Center: one DV mounted to spectrograph and one DV behind an integrating sphere during flat fielding. Right: ESO transport container with 2 DVs packed for shipment.

The major test consists of a focus series, with the DV mounted at the spectrograph #3. The MUSE spectrographs are designed to be very stable systems with a fixed spectral format and no movable parts. The exception to this is a mechanical focus stage between spectrograph and detector vessel that can be adjusted manually and in piston only. As this focus stage is unsuitable to perform automated serial testing, a motorized pinhole illumination unit at the entrance is moved instead. Part of the test bench validation was to verify that moving the pinhole mask at the object plane provides similar results than moving the detector at the image plane. The IU is moved 2.5mm through focus which corresponds to the available focal range of 400 microns at the MUSE spectrograph. This focus series also re-confirmed the magnification of the system of 6.45. The best focus can be determined with an accuracy of 100 µm (at the IU plane) which corresponds to 15 µm at the detector plane.

5.4 Analyses and Results

The dispersed images of the 11 pinholes along the spatial direction (slices) illuminated with Hg+Ne+Xe spectral lamps result in over 500 spots across the CCD. After the raw frames were dark subtracted, all emission spots above a certain threshold are detected and wavelength correlated. As the images of the pinholes are under-sampled at the detector, the determination of the encircled energy is non-trivial. A window of 11x11 pixel is placed around each PSF, then enlarged

by a factor of 10 and afterwards the spot is interpolated (to minimize artifacts, a Lanczos kernel was chosen). This enlarged, interpolated image of the spot (Fig. 7 right) is then used to determine the A80 ensquared energy. The A80 value is defined as the length of one side of a square which has to contain 80% of the total flux of the spot.

The A80 values were calculated for all spots across the chip at all focal positions. The resulting focus curves yield the best overall focus (= minimum of A80 values in Fig. 9 left), the best focus at a particular wavelength region (465-600nm; 600-800nm; 800-870nm, see Fig. 5 left) and best focus versus spatial direction (0-200pxl: 1900-2200pxl; 3800-4100pxl, see Fig. 10 right). The dependency of the best focus value across the CCD x- and y-direction was used to calculate the tip/tilt (Fig. 11) of the detector plane versus the optical axis of the spectrograph.

Finally, the locations of the spots on the CCD were measured and provided the lateral shift (dx and dy) and the rotation of a DV under test (see Fig 9, right) with respect to a reference frame (DV22). As example, table 1 summarizes the test results for a particular DV (#19) versus their respective specifications as set by the instrument requirements.

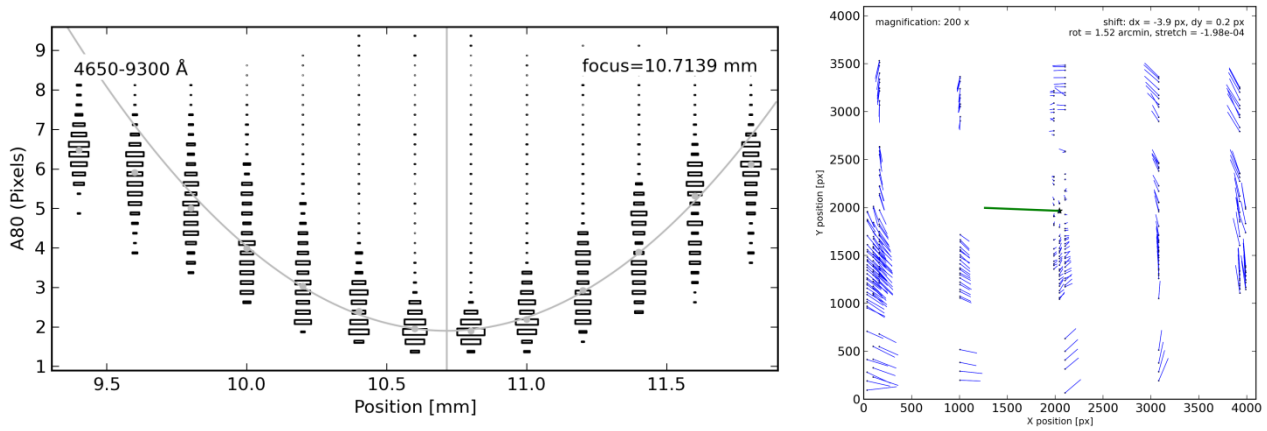

Figure 9. Left: A80 distribution versus focus position for the whole CCD. The histogram bins of the A80 distribution for every focus position are shown as boxes with an area proportional to the content (i.e., number of elements) in the bin. All histogram entries are weighted with the estimated A80 flux and normalized to 1.0 for one focus position. The quadratic fit of the best focus position is shown as curve in the diagram. Right: Displacement of the spots with respect to a reference frame taken with DV22. For a central spot position, its relative shift between the images is shown by a thick green line. For each spot position that appears in both images, the displacement additionally to the central shift is shown as blue lines, indicating a rotation. (Note: these lines are magnified by a factor of 200 for better visibility).

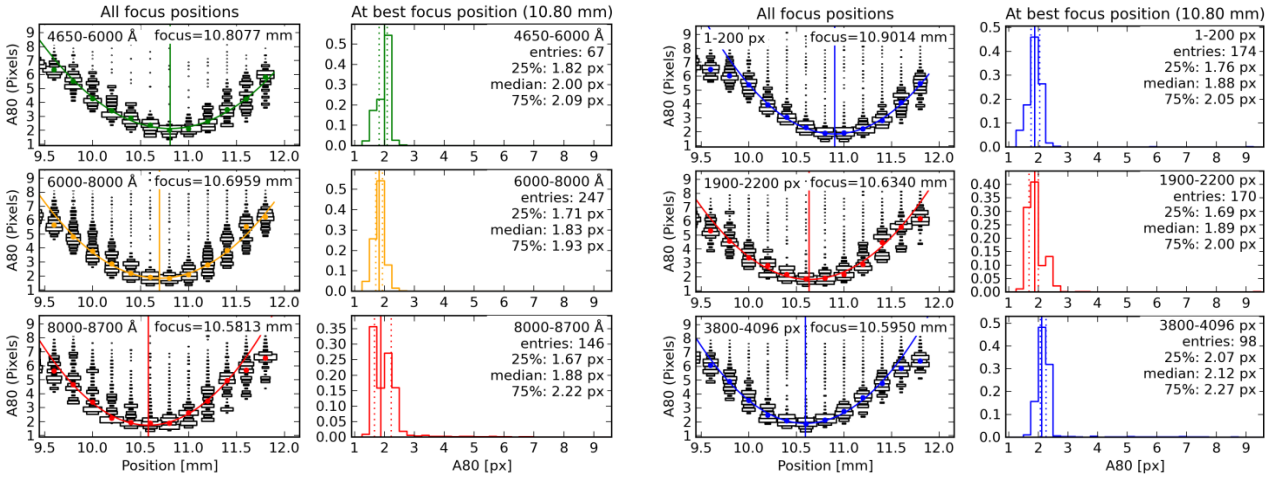

Figure 10. Left: A80 distribution versus focus position for the three wavelength ranges (focus curve vs. color). The adjacent diagram shows the normalized histogram for the common best focus. Right: A80 distribution versus focus positions for three spatial areas (left, center and right part of the CCD, i. e. focus curve vs. off-axis).

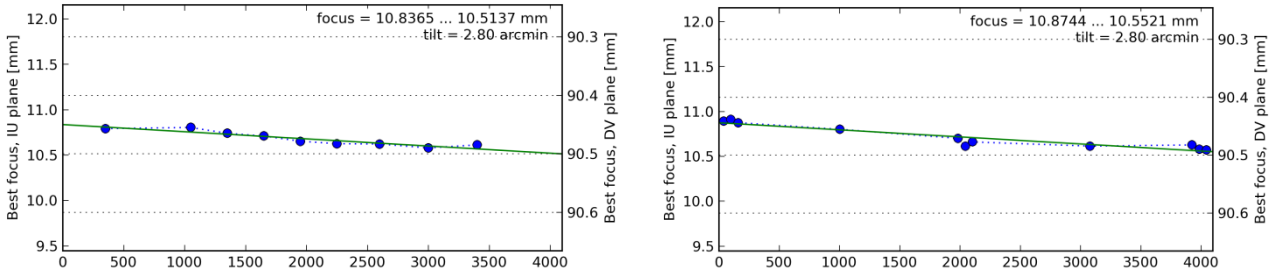

Figure 11. Left: Dependency of the best focus position in the dispersion direction. Right: Dependency of the best focus position in the spatial direction. The spectrograph magnification used to calculate the tip and tilt is 6.45.

Table 1. Compliance matrix of measured parameters versus specifications (example for DV19).

Parameter	**Measurement**	**Specification**	**Compliance**
A80 (“Blue”, 465-600nm)	1.65 pixel	≤ 2.08 pixel	Yes
A80 (“Middle”, 600-800nm)	1.41 pixel	≤ 1.72 pixel	Yes
A80 (“Red”, 800-870nm)	1.48 pixel	≤ 1.61 pixel	Yes
X (spatial) Tilt	2.80 arcmin	(2.5 ± 2.0) arcmin	Yes
Y (dispersion) Tilt	2.80 arcmin	(2.0 ± 2.0) arcmin	Yes
DV Rotation	1.52 arcmin	≤ ±2.5 arcmin	Yes
DV X-shift	-58 µm	≤ ±70 µm	Yes
DV Y-shift	2 µm	≤ ±70 µm	Yes
DV Focus (Z) shift	-13 µm	≤ ±50 µm	Yes

5.5 Comparison of detectors

With the results of almost all tested MUSE detectors (24 regular DVs + 1 spare + 1 for reference), the distribution of measured parameters gives an indication about the integration accuracy and alignment reproducibility of the entire series. Plots with the measured x/y-shifts (Fig. 12, left) and the tip/tilts (Fig. 12, right) of the detector plane versus the optical axis of the SPS3 spectrograph are shown below.

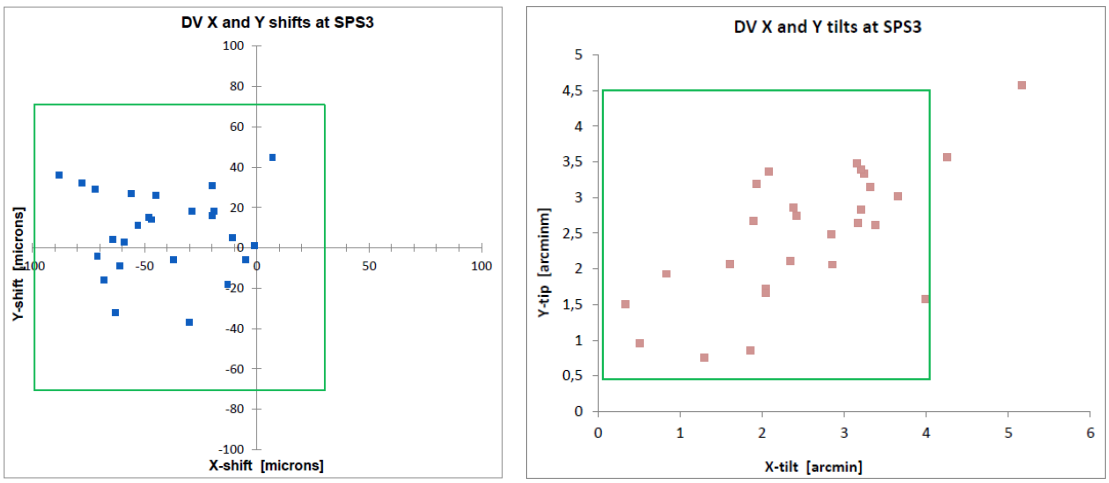

Figure 12. Plot of the lateral shifts (left) and the tip/tilt (right) of the detector plane with respect to the optical axis of spectrograph SPS3. While the square boxes indicate the system requirements, all DVs could be aligned within spec in the final IFU setup.

When comparing the best focus positions obtained with the IU and SPS3 at the test bench with the mechanical alignment of the CCD chip at ESO (Fig. 13 left) or the focus setting in the final IFU configuration (including image slicer, Fig. 13 right), there is no strong correlation. Given that these tests measure different parameters under different configurations this is little surprising though.

Nevertheless, the conclusion of the described DV acceptance testing is that the series of 24 detectors could be built within tight tolerances and yielded the good image qualities and geometrical alignments as required for the MUSE instrument.

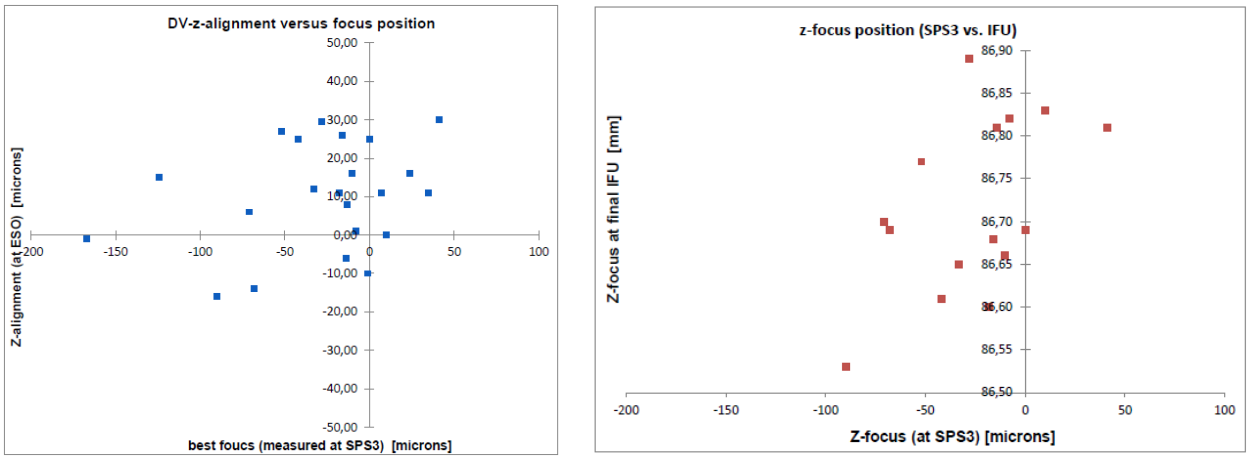

Figure 13. Left: plot of the mechanical z-alignment of the CCD vs. the best focus values obtained with the test bench setup. Right: plot of best focus values obtained with the test bench and SPS3 versus the final alignment using various IFUs.

6. AKNOWLEDGEMENTS

The authors wish to thanks the complete MUSE project team for the fruitful cooperation and the project management (R. Bacon and P. Callier) for the trust in the VCS team. We would also like to thank Eric Mueller for his work on the support and analysis software for the CPMM.

REFERENCES

1. http://www.eso.org/sci/facilities/develop/integration/
2. Lizon, J.L., Accardo, M., “LN2 continuous flow cryostats: a compact vibration free cooling system for single or multiple detector systems”, Proc. SPIE, 7739, 7739E
3. Bacon, R., et al., "The MUSE second generation VLT instrument ", Proc. SPIE 7735, 773508-9 (2010).
4. Kelz, A.; Bauer, S. M.; Biswas, I.; Fechner, T.; Hahn, T.; Olaya, J.-C.; Popow, E.; Roth, M. M.; Streicher, O.; Weilbacher, P.; Bacon, R.; Laurent, F.; Laux, U.; Lizon, J. L.; Loupias, M.; Reiss, R.: Rupprecht, G., "The calibration unit and detector system tests for MUSE ", Proc. SPIE 7735, 773552-12 (2010).
5. Laurent, F.; et al., "MUSE integral field unit: test results on the first out of 24", Proc. SPIE 7739 (2010).